



Comparison of the magnetic fields in solar active regions derived with different instruments

R. Suleymanova

Crimean Astrophysical Observatory, Nauchny 298409
e-mail: bictr97@gmail.com

Received 15 June 2022

ABSTRACT

The paper presents a comparison of the magnetic fluxes in active regions (ARs) measured with SOHO/MDI and SDO/HMI. The transition coefficients from HMI to MDI data are as follows: 1.46 for ARs observed within 10° of the central meridian and 1.29 for ARs observed at longitudes $[-60^\circ; -10^\circ]$ and $[10^\circ; 60^\circ]$. The maximum magnetic field values in sunspots obtained in 2014 from SDO/HMI and with the ground-based telescope BST-2 at the Crimean Astrophysical Observatory of the Russian Academy of Sciences were compared using the orthogonal regression method. It is shown that the best agreement between data from the two instruments is achieved when comparing Crimean data with HMI data on the full field vector (correlation coefficient 0.71) rather than on its longitudinal component (correlation coefficient 0.66). This conclusion indicates that the field measurements by the spectral line shift method (applied at BST-2) yield a value of the full field vector with the sign of its longitudinal component. The comparison results evidence for the possibility of using Crimean sunspot magnetic field data, which is particularly valuable for studying solar cycles prior to the space age.

Key words: Sun, magnetic fields

1 Introduction

The magnetic field of the Sun determines solar activity, manifesting itself in the formation and evolution of sunspots, in the existence of a solar cycle. It is responsible for eruptive processes such as flares and coronal mass ejections, as well as for extended periods of solar inactivity, such as global activity minima. All these factors influence space weather in the vicinity of our planet. Therefore, it is important to study the solar magnetic field over long homogeneous time intervals. Reliable measurements of solar magnetic fields from space have been available since 1996 when the first images of the solar disk were captured by the Solar and Heliospheric Observatory/Michelson Doppler Imager (SOHO/MDI) (Scherrer et al., 1995). Magnetographic data obtained by the Solar Dynamics Observatory/Helioseismic and Magnetic Imager (SDO/HMI) instrument have been accessible since 2010 (Scherrer et al., 2012). A long homogeneous dataset for earlier years is of particular scientific interest. In this regard, it is possible to use data from the BST-2 telescope at the Crimean Astrophysical Observatory of the Russian Academy of Sciences (CrAO RAS) where the measurements of maximum magnetic fields in sunspots have been carried out since 1956 using the unified methodology. To achieve this, it is necessary to investigate the compatibility of data from MDI, HMI, and the BST-2 telescope, which is the main objective of this study.

2 Data and methods

This study makes use of data from the instruments such as SDO/HMI (Liu et al., 2012; Schou et al., 2012), SOHO/MDI (Scherrer et al., 1995), and the BST-2 telescope (Severnyi, Stepanov, 1956) at CrAO RAS.

The Helioseismic and Magnetic Imager (HMI) is part of the Solar Dynamics Observatory (SDO). This instrument functions as a filtergraph capturing the full disk of the Sun with a spatial resolution of $1''$ and a pixel size of $0.5'' \times 0.5''$. Magnetic field measurements are taken in the absorption line of Fe I 6173 Å. Since line-of-sight (LOS) magnetograms are required to compare magnetic fluxes from HMI and MDI, the data from the front camera are used in this study (for a more detailed description, see Schou et al., 2012; Liu et al., 2012). The set of filtergrams from this camera is constructed from the series of images taken at six points along the spectral line under two different polarization states (Schou et al., 2012).

For comparison with data from the BST-2 telescope, magnetograms from the side camera are used (for a more detailed description, see Schou et al., 2012; Liu et al., 2012), as it produces a series of images at six points along the spectral line under six different polarization states. This allows one to obtain magnetograms of the full magnetic field vector. The magnetograms ready for scientific analysis are freely avail-

able on the official website of the Joint Science Operations Center (JSOC¹).

The Michelson Doppler Imager (MDI), predecessor of the SDO instrument, is part of the Solar and Heliospheric Observatory (SOHO). This instrument also functions as a filtergraph capturing the full disk of the Sun with a resolution of 4'' and a pixel size of 2'' × 2'' (Scherrer et al., 1995). At four points along the Ni I 6768 Å absorption line, four filtergrams are constructed to generate a map of Doppler velocities on the solar disk. The LOS magnetograms are obtained by differencing dopplergrams of right and left circular polarizations. These data are freely available and provided by JSOC².

The solar tower telescope BST-2 is an operating solar telescope at CrAO RAS. It has been used for solar observations and measuring maximum magnetic fields of sunspots since 1956. By using the Zeeman effect, the splitting of the Fe I 6302 Å line is observed. An analyzer, which consists of a quarter-wave plate and a polaroid mosaic, is positioned just before the spectrograph slit to isolate right and left circular polarizations. The quarter-wave plate converts circular polarization into linear polarization, while the mosaic alternately selects mutually perpendicular directions of linearly polarized light. By measuring the distance of deviation from the central iron line, the maximum magnetic field of sunspots can be determined (Severnyi, Stepanov, 1956).

Since the spectral line splitting depends solely on the atom's properties and the absolute value of the magnetic field, whereas the magnetic field vector's orientation relative to the observer is determined by the polarization and amplitude of spectral components, it can be suggested that by using BST-2 the full magnetic field vector modulus is measured by the deviation from the central line, while its sign is determined by the direction of deviation (to the right or left) from the central line (Plotnikov, Kutsenko, 2018). The accuracy of magnetic field measurements is 100 Mx cm⁻². Magnetic fields below 1000 Mx cm⁻² cannot be measured with sufficient accuracy. The measurement data are publicly available on the CrAO RAS website³ in the form of sketches.

One of the results in Biktimirova, Abramenko (2020) is the digitized values of the magnetic fields of sunspots measured with BST-2 in 2014. We made use of these data here.

2.1 Relation between the magnetic fluxes measured with MDI and HMI

Liu et al. (2012) performed a pixel-by-pixel comparison of the magnetic fields measured with MDI and HMI in the way as follows. The resolution of HMI magnetograms was reduced to that of MDI using Gaussian smoothing. For each MDI magnetogram, distortion correction and positional angle offset were carried out. Corrected MDI magnetograms were used to calculate the rotation angles of HMI magnetograms. Blurred and rotated HMI magnetograms, compared pixel by pixel with MDI magnetograms, served as a proxy

magnetogram. The obtained proxy magnetogram was compared with the MDI magnetogram, considering pixels not further than 60° from the center of the Sun. The relation between the magnetic field values was obtained as

$$B_{\text{LOS}}(\text{MDI}) = -0.18 + 1.40B_{\text{LOS}}(\text{HMI}),$$

where $B_{\text{LOS}}(\text{MDI})$ and $B_{\text{LOS}}(\text{HMI})$ are in Mx cm⁻². The authors further compared different regions of the solar disk using the same data as in the previous comparison. Pixels were taken in three zones: [-30°; 30°] and [30°; 45°], [45°; 70°] on both sides of the central meridian, resulting in transition coefficients of 1.43, 1.40, and 1.26, respectively. The authors concluded that the transition coefficient between the magnetic field data measured with MDI and HMI varies depending on the distance from the center of the disk.

A comparison was also made between the magnetic fluxes measured with MDI and HMI. Twenty-three active regions near the central meridian (10° in longitude) and 23 active regions at longitudes [-60°; -10°] and [10°; 60°] were selected. Each region was individually cropped from the full-disk LOS magnetograms of MDI and HMI to ensure that both images were as similar as possible, i.e., covering the same area on the disk. When calculating the magnetic fluxes, correction for the projection effect (μ correction, Hagenaar, 2001) was only applied to active regions at longitudes [-60°; -10°] and [10°; 60°].

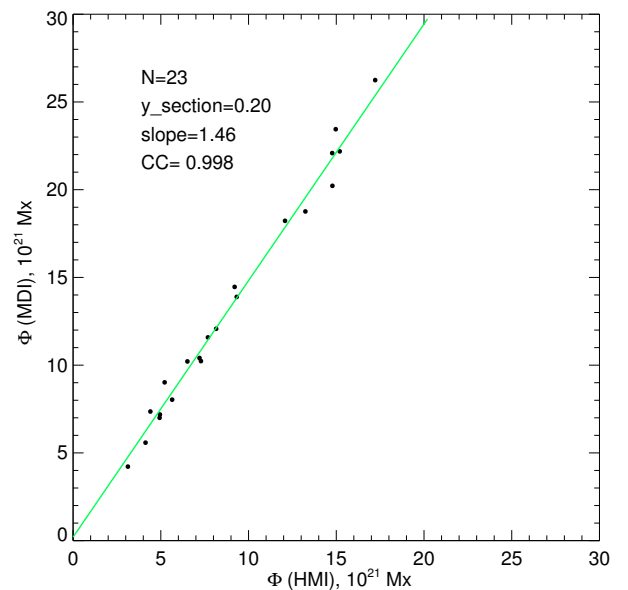


Fig. 1. Graph of the relation between the magnetic fluxes of active regions near the central meridian; $\Phi(\text{MDI})$ (along the Oy axis) and $\Phi(\text{HMI})$ (along the Ox axis).

The relation between magnetic fluxes for active regions near the central meridian was determined as

$$\Phi(\text{MDI}) = (0.22 \pm 0.28) + (1.46 \pm 0.02)\Phi(\text{HMI}),$$

where $\Phi(\text{MDI})$ and $\Phi(\text{HMI})$ are in units of 10^{21} Mx. The correlation coefficient is 0.998 with a 95% confidence in-

¹ <http://hmi.stanford.edu/magnetic/>

² http://jsoc.stanford.edu/MDI/MDI_Magnetograms.html

³ <https://sun.crao.ru/observations/sunspots-magnetic-field>

terval of 0.97–0.99. The resulting linear regression plot is shown in Fig. 1.

For active regions at longitudes $[-60^\circ; -10^\circ]$ and $[10^\circ; 60^\circ]$, the relation between magnetic fluxes was obtained as

$$\Phi(\text{MDI}) = (0.56 \pm 0.69) + (1.29 \pm 0.03)\Phi(\text{HMI}),$$

where $\Phi(\text{MDI})$ and $\Phi(\text{HMI})$ are in units of 10^{21} Mx. The correlation coefficient is 0.992 with a 95% confidence interval of 0.97–0.99. The linear regression plot is shown in Fig. 2.

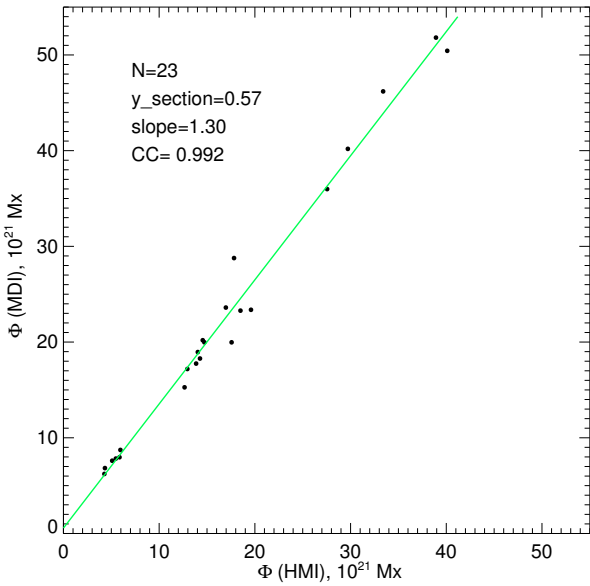


Fig. 2. Graph of the relation between the magnetic fluxes of active regions at longitudes $[-60^\circ; -10^\circ]$ and $[10^\circ; 60^\circ]$; $\Phi(\text{HMI})$ (along the Oy axis) and $\Phi(\text{HMI})$ (along the Ox axis).

The comparison of magnetic fluxes in this study is coincident with the conclusions drawn by Liu et al. (2012). The transition coefficient between the magnetic fluxes measured with MDI and those measured with HMI varies depending on the distance from the center of the Sun to its limb: 1.46 at the center of the solar disk and 1.29 at the edge of the solar disk.

2.2 Relation between the maximum magnetic fields measured with BST-2 and HMI

To confirm that the BST-2 telescope measures the full magnetic field vector (Plotnikov, Kutsenko, 2018), a comparison was performed between the absolute values of the maximum magnetic field measured with BST-2 and those measured with HMI: the longitudinal component of the magnetic field and the full magnetic field vector. Active regions at the center of the solar disk (within 14° from the central pixel) and active regions at longitudes $[-60^\circ; -40^\circ]$ and $[40^\circ; 60^\circ]$ were considered. As both sets of measurements (BST-2 and HMI) are burdened with errors, following the methodology presented in Nagovitsyn et al. (2016), orthogonal regression was applied.

This method allows one to calculate the coefficients of linear dependence

$$\zeta = m + b\theta$$

under the assumption that both sets are burdened with errors. Here θ represents the series of magnetic field measurements obtained at CrAO, and ζ represents the series of magnetic field measurements acquired with HMI. Details of the method can be found in Nagovitsyn et al. (2016). The calculations were performed using the IDL programming environment with the sixlin.pro function.

For active regions near the solar disk, the relation between the longitudinal components of the magnetic field measured with HMI and the magnetic fields measured with BST-2 is as follows:

$$B_{\text{LOS}}(\text{HMI}) = (213 \pm 394) + (0.88 \pm 0.22)B(\text{CR}),$$

where $B_{\text{LOS}}(\text{HMI})$ and $B(\text{CR})$ are in units of Mx cm^{-2} . The correlation coefficient is 0.66 with a 95% confidence interval of 0.54–0.75. Following the notations in Nagovitsyn et al. (2016), the Crimean measurements are denoted as $B(\text{CR})$.

For the dependence of the full magnetic field vectors measured with HMI on the magnetic fields measured with BST-2, the relation can be written as

$$B(\text{HMI}) = (277 \pm 349) + (0.92 \pm 0.19)B(\text{CR}),$$

where $B(\text{HMI})$ and $B(\text{CR})$ are in units of Mx cm^{-2} . The correlation coefficient is 0.71 with a 95% confidence interval of 0.59–0.79.

Table 1. Correlation coefficients, slopes, and free terms of orthogonal regression obtained by comparing the magnetic fields of sunspots at the center of the disk: HMI longitudinal component data versus BST-2 data (second column), HMI full vector data versus BST-2 data (third column).

Quantity	$B_{\text{LOS}}(\text{HMI})$ vs $B(\text{CR})$	$B(\text{HMI})$ vs $B(\text{CR})$
Number of measurements, N	103	103
Correlation coefficient, CC	0.66	0.71
Free term, y_section (Mx cm^{-2})	213 ± 394	277 ± 349
Slope	0.88 ± 0.22	0.92 ± 0.19

The number of measurements, correlation coefficients, slopes, and free terms of orthogonal regression for active regions at the center of the solar disk are provided in Table 1. Figure 3 shows the graph of the relation between the longitudinal components of the magnetic field measured with HMI and the magnetic fields measured with BST-2. Figure 4 shows the graph of the relation between the full magnetic field vectors measured with HMI and the magnetic fields measured with BST-2.

For active regions at longitudes $[-60^\circ; -40^\circ]$ and $[40^\circ; 60^\circ]$, the relation between the longitudinal components of the magnetic field measured with HMI and the magnetic fields measured with BST-2 is as follows:

$$B_{\text{LOS}}(\text{HMI}) = (-278 \pm 137) + (0.94 \pm 0.08)B(\text{CR}),$$

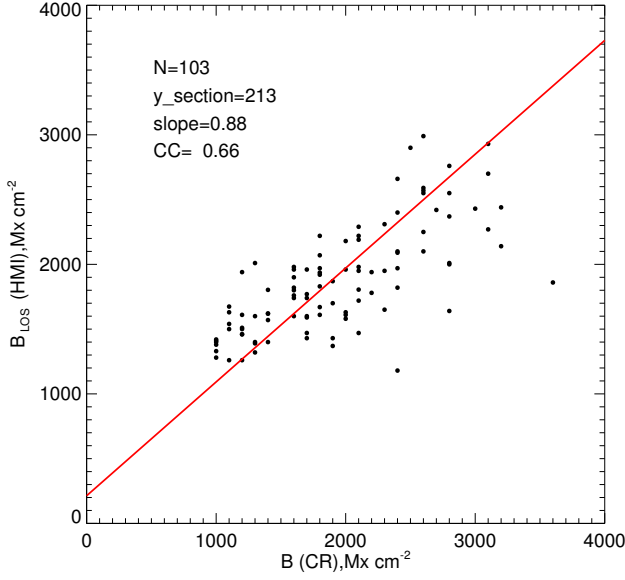


Fig. 3. Graph of the dependence of the absolute values of magnetic fields at the center of the solar disk $B_{\text{LOS}}(\text{HMI})$ on $B(\text{CR})$.

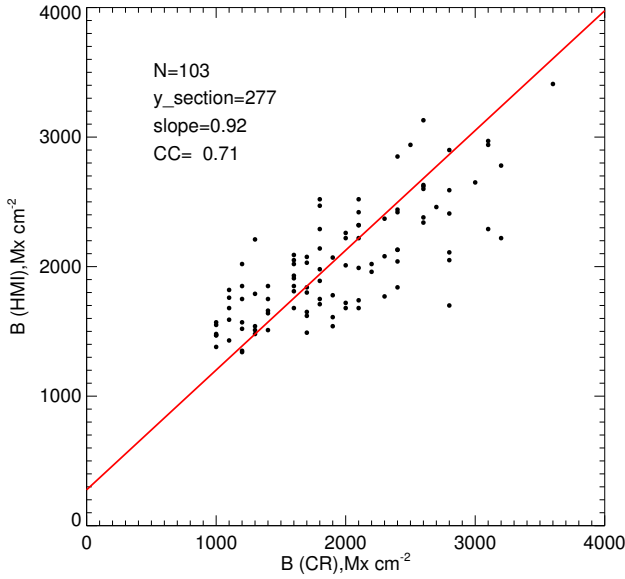


Fig. 4. Graph of the dependence of the absolute values of magnetic fields at the center of the solar disk $B(\text{HMI})$ on $B(\text{CR})$.

where $B_{\text{LOS}}(\text{HMI})$ and $B(\text{CR})$ are in units of Mx cm^{-2} . The correlation coefficient is 0.73 with a 95% confidence interval of 0.63–0.80.

Regarding the dependence of the full magnetic field vectors measured with HMI on the magnetic fields measured with BST-2, the relation is described as

$$B(\text{HMI}) = (341 \pm 190) + (0.99 \pm 0.12)B(\text{CR}),$$

where $B(\text{HMI})$ and $B(\text{CR})$ are in units of Mx cm^{-2} . The correlation coefficient is 0.76 with a 95% confidence interval of 0.66–0.82.

Table 2. Correlation coefficients, slopes, and free terms of orthogonal regression obtained by comparing the magnetic fields of sunspots at longitudes $[-60^\circ; -40^\circ]$ and $[40^\circ; 60^\circ]$: HMI longitudinal component data versus BST-2 data (second column), HMI full vector data versus BST-2 data (third column).

Quantity	$B_{\text{LOS}}(\text{HMI})$ vs $B(\text{CR})$	$B(\text{HMI})$ vs $B(\text{CR})$
Number of measurements, N	115	115
Correlation coefficient, CC	0.73	0.71
Free term, y_{section} (Mx cm^{-2})	-278 ± 137	341 ± 190
Slope	0.94 ± 0.08	0.99 ± 0.12

The number of measurements, correlation coefficients, slopes, and free terms of orthogonal regression for active regions at longitudes $[-60^\circ; -40^\circ]$ and $[40^\circ; 60^\circ]$ are provided in Table 2. Figure 5 shows the graph of the relation between the longitudinal components of the magnetic field measured with HMI and the magnetic fields measured with BST-2. Figure 6 shows the graph of the relation between the full magnetic field vectors measured with HMI and the magnetic fields measured with BST-2.

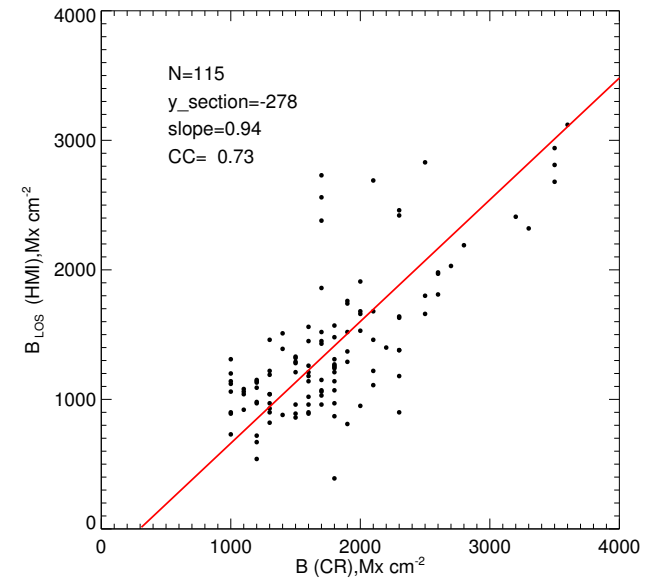


Fig. 5. Graph of the dependence of the absolute values of magnetic fields at longitudes $[-60^\circ; 40^\circ]$ and $[40^\circ; 60^\circ]$ $B_{\text{LOS}}(\text{HMI})$ on $B(\text{CR})$.

The calculations above have shown that the correlation coefficient for the relation between the full magnetic field vectors measured with HMI and the maximum magnetic fields measured with BST-2 is always greater than the correlation coefficient for the relation between the longitudinal components of the magnetic field measured with HMI and the maximum magnetic fields measured with BST-2. We can draw a conclusion that the BST-2 telescope can measure a full magnetic field vector.

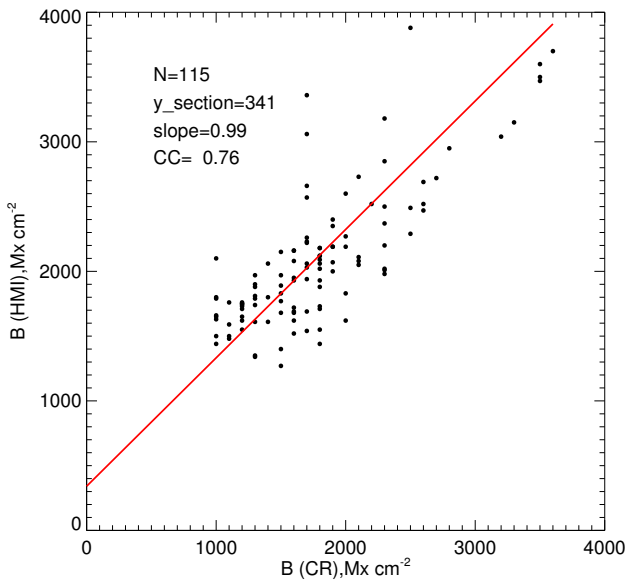


Fig. 6. Graph of the dependence of the absolute values of magnetic fields at longitudes $[-60^\circ; -40^\circ]$ and $[40^\circ; 60^\circ]$ $B(\text{HMI})$ on $B(\text{CR})$.

Nagovitsyn et al. (2016) performed a comparison of the magnetic fields of sunspots measured at CrAO RAS and other ground-based observatories (including, for example, the Mount Wilson Observatory, IZMIRAN, the Special Astrophysical Observatory of the Russian Academy of Sciences, etc.). The authors obtained comparison graphs and transition equations using the orthogonal regression method. The comparison graphs obtained in our work belong to the same class of accuracy.

Furthermore, the good agreement between the data from the HMI instrument and those from the BST-2 telescope allows us to state that the data on the magnetic fields of sunspots can be used in further research.

3 Conclusions

We have performed a comparison of data on magnetic fluxes measured with MDI and HMI instruments. Comparisons were also made between the magnetic fields of sunspots measured with HMI and BST-2.

The relation between magnetic fluxes of active regions observed near the central meridian is $\Phi(\text{MDI}) = 0.22 + 1.46 \Phi(\text{HMI})$. For active regions at longitudes $[-60^\circ; -10^\circ]$ and $[10^\circ; 60^\circ]$, the analogous relation is $\Phi(\text{MDI}) = 0.56 + 1.29 \Phi(\text{HMI})$.

Thus, the transition coefficient between the magnetic flux data from MDI and HMI for active regions near the central meridian is 1.46, and for sunspots at longitudes $[-60^\circ; -10^\circ]$ and $[10^\circ; 60^\circ]$ it is 1.29.

Correlation coefficients were obtained when comparing the absolute values of maximum magnetic fields in sunspots measured with HMI (longitudinal component of the magnetic field and full magnetic field vector) and values of maximum magnetic fields measured with BST-2. These coefficients confirm that the BST-2 telescope can measure the maximum values of the full magnetic field vector.

It is concluded that the comparison results of magnetic field measurements obtained with BST-2 (CrAO RAS) and SDO/HMI complement the comparison results obtained in Nagovitsyn et al. (2016).

The high degree of correlation (0.73) between BST-2 and HMI data suggests that the data on maximum magnetic fields in sunspots measured with BST-2 can be used to extend a homogeneous series of sunspot magnetic field measurements into the pre-space era.

Acknowledgments. The author is grateful to Dr. Yu.A. Nagovitsyn and Dr. V.I. Abramenko for discussions and a number of valuable suggestions. The comparison of HMI and MDI data was supported by the Russian Science Foundation grant (project 18-12-00131); the comparison of HMI and CrAO RAS data was supported by the research plan of the Federal State Budgetary Scientific Institution “Crimean Astrophysical Observatory of the Russian Academy of Sciences” 1021051101548-7-1.3.8.

References

- Biktimirova R.A., Abramenko V.I., 2020. *Izv. Krymsk. Astrofiz. Observ.*, vol. 116, no. 1, pp. 7–13. (In Russ.)
- Nagovitsyn Yu.A., Pevtsov A.A., Osipova A.A., et al., 2016. *Pis'ma Astron. Zh.*, vol. 42, no. 10, pp. 773–782. (In Russ.)
- Plotnikov A.A., Kutsenko A.C., 2018. *Izv. Krymsk. Astrofiz. Observ.*, vol. 114, no. 2, pp. 87–96. (In Russ.)
- Severnyi A.B., Stepanov V.E., 1956. *Izv. Krymsk. Astrofiz. Observ.*, vol. 16, pp. 3–11. (In Russ.)
- Hagenaar H.J., 2001. *Astrophys. J.*, vol. 555, no. 1, pp. 448–461.
- Liu Y., Hoeksema J.T., Scherrer P.H., et al., 2012. *Solar Phys.*, vol. 279, pp. 295–316.
- Scherrer P.H., Bogart R.S., Bush R.I., et al., 1995. *Solar Phys.*, vol. 162, pp. 129–188.
- Scherrer P.H., Schou J., Bush R.I., et al., 2012. *Solar Phys.*, vol. 275, pp. 207–227.
- Schou J., Scherrer P.H., Bush R.I., et al., 2012. *Solar Phys.*, vol. 275, pp. 229–259.